



Deposited via The University of Sheffield.

White Rose Research Online URL for this paper:

<https://eprints.whiterose.ac.uk/id/eprint/127645/>

Version: Accepted Version

Article:

Cullen, W., Metherell, A.J., Wragg, A.B. et al. (2018) Catalysis in a Cationic Coordination Cage Using a Cavity-Bound Guest and Surface-Bound Anions: Inhibition, Activation, and Autocatalysis. *Journal of the American Chemical Society*, 140 (8). pp. 2821-2828. ISSN: 0002-7863

<https://doi.org/10.1021/jacs.7b11334>

Reuse

Items deposited in White Rose Research Online are protected by copyright, with all rights reserved unless indicated otherwise. They may be downloaded and/or printed for private study, or other acts as permitted by national copyright laws. The publisher or other rights holders may allow further reproduction and re-use of the full text version. This is indicated by the licence information on the White Rose Research Online record for the item.

Takedown

If you consider content in White Rose Research Online to be in breach of UK law, please notify us by emailing eprints@whiterose.ac.uk including the URL of the record and the reason for the withdrawal request.

Catalysis in a cationic coordination cage using a cavity-bound guest and surface-bound anions: inhibition, activation and autocatalysis.

William Cullen,^a Alexander J. Metherell,^a Ashley B. Wragg,^a Christopher G. P. Taylor,^b Nicholas H. Williams,^{a,*} and Michael D. Ward^{a,b,*}

^a Department of Chemistry, University of Sheffield, Sheffield S3 7HF, UK.

^b Department of Chemistry, University of Warwick, Coventry CV4 7AL, UK.

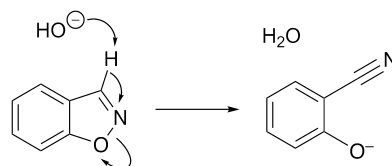
ABSTRACT: The Kemp elimination (reaction of benzisoxazole with base to give 2-cyanophenolate) is catalyzed in the cavity of a cubic M_8L_{12} coordination cage because of a combination of (i) benzisoxazole binding in the cage cavity driven by the hydrophobic effect, and (ii) accumulation of hydroxide ions around the 16+ cage surface driven by ion-pairing. Here we show how reaction of the cavity-bound guest is modified by the presence of other anions which can also accumulate around the cage surface and displace hydroxide, inhibiting catalysis of the cage-based reaction. Addition of chloride or fluoride inhibits the reaction with hydroxide to the extent that a new autocatalytic pathway becomes apparent, resulting in a sigmoidal reaction profile. In this pathway the product 2-cyanophenolate itself accumulates around the cationic cage surface, acting as the base for the next reaction cycle. The affinity of different anions for the cage surface is therefore 2-cyanophenolate (generating autocatalysis) > chloride > fluoride (which both inhibit the reaction with hydroxide but cannot deprotonate the benzisoxazole guest) > hydroxide (default reaction pathway). The presence of this autocatalytic pathway demonstrates that a reaction of a cavity-bound guest can be induced with different anions around the cage surface in a controllable way; this was confirmed by adding different phenolates to the reaction, which accelerate the Kemp elimination to different extents depending on their basicity. This represents a significant step towards the goal of using the cage as a catalyst for bimolecular reactions between a cavity-bound guest and anions accumulated around the surface.

INTRODUCTION

The ability of hollow container molecules to bind small molecules or ions as guests in their central cavity¹⁻⁵ has led to a wide range of possible applications² from drug uptake / release³ to photocatalysis.⁴ Prominent amongst these properties are examples where binding alters the reactivity of guests, and include reactions of bound guests that are catalysed with rate enhancements of several million fold in the best cases.⁵

There are various mechanisms by which catalysis can occur in the cavity of a synthetic host, with both cavity shape/size and the charge of the host playing important roles in different cases. Both Rebek⁶ and Fujita⁷ showed how co-encapsulation of the two different components of a Diels-Alder reactions can lead to accelerated reactions, with the catalysis arising from the enforced proximity of the reactants – an increase in the effective concentration of each species around the other. In Fujita's example this led to altered regioselectivity due to the relative orientation of the two components in the constricted environment inside the cage cavity.⁷ In a conceptually similar way, the 'constrictive binding' of an open-chain substrate containing alkene and amine functionalities led to an unexpected Aza-Prins cyclisation pathway promoted by folding of the substrate when it bound in a host cavity, giving a product that was not observed in the normal solution-phase reaction.⁸ The importance of the charge of the host has been demonstrated by numerous examples from the Raymond/Bergman group of

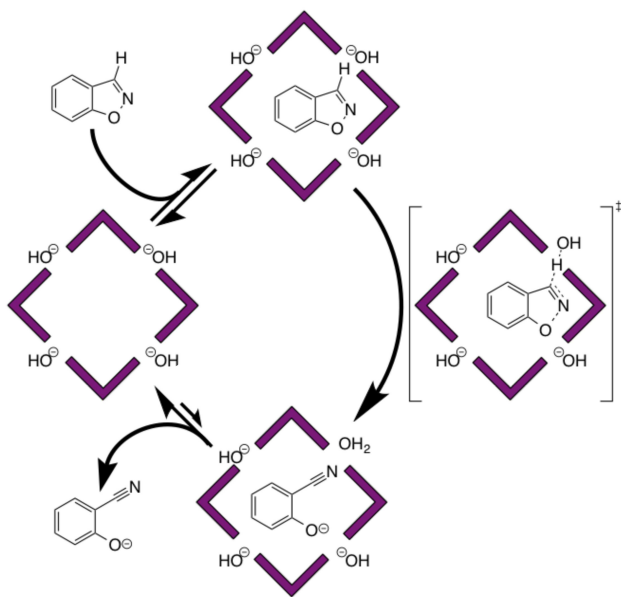
catalysis by a tetrahedral cage which carries a high negative charge (12-).^{9,10} For example, this negative charge helps to stabilise the cationic intermediate involved in a Nazarov cyclisation of a dienol to a cyclopentadiene, contributing to the 10⁶-fold rate acceleration observed.⁹ Similarly, the ability of the high negative charge of this cage to stabilise cationic guests enables the protonation of cavity-bound guests even in base, allowing acid-catalysed reactions to occur under these conditions.¹⁰



Scheme 1. The Kemp elimination reaction: deprotonation of benzisoxazole at the 3-position leading to ring-opening and formation of 2-cyanophenolate.

We recently reported efficient (2×10^5 -fold) catalysis of the Kemp elimination¹¹ – the base promoted conversion of benzisoxazole to 2-cyanophenolate (Scheme 1)¹² – when the benzisoxazole is bound in the cavity of an approximately cubic M_8L_{12} coordination cage. The proposed catalytic cycle is shown in Scheme 2. We ascribed the catalytic effect to the

16+ charge on the cage, arising from the eight Co^{2+} ions at the vertices. This high positive charge results in accumulation of hydroxide ions around the cage surface, affording a very high local concentration of hydroxide ions close to the bound guest in the cavity. The effect is sufficiently strong that when the bulk solution was at pD 8.5, the bound guest underwent the Kemp elimination at the same rate as when it was free in solution at pD 13.8.¹¹ The ability of our cationic cage to accumulate anions around its surface was shown by a control experiment using competing anions:¹¹ in the presence of an excess of chloride ions, the catalysis was switched off and the benzisoxazole reacted at only the background rate, even though (i) it remained bound in the cage cavity and (ii) chloride does not itself directly interfere with the Kemp elimination.¹² This effect was ascribed to the fact that chloride ions, being more easily desolvated than hydroxide ions,¹³ would preferentially bind to the cage surface and thereby displace the hydroxide ions from their proximity to the substrate. This observation is important as it suggests that a wide range of different types of anion might accumulate around the cage in water, especially ‘soft’ anions that are weakly solvated: this, in turn, could provide a mechanism to surround any of a wide range of guests^{3d,14} with a high local concentration of a selected anion, using two orthogonal interactions. As guest binding in the cavity (lined with CH groups from the ligands) contains a substantial contribution from the hydrophobic effect,^{14,15} and accumulation of anions around the cationic cage is based on a polar interaction (ion-pairing),¹¹ it should be possible to vary the two independently of one another – leading to the ability to control a wide range of cage-catalysed reactions of hydrophobic electrophilic guests with surface-bound anions.



Scheme 2. Sketch of the cage-catalysed catalytic reaction cycle, based on accumulation of hydroxide ions around the cationic cage surface (reproduced with permission from ref. 11).

In this work we have explored how the cage-catalysed Kemp elimination is inhibited by a range of anions, which unexpectedly revealed autocatalytic behaviour by the system. This in turn has led to us to observe that the catalytic activity of the cage for the reaction of cavity-bound benzisoxazole with a surface-bound basic anion shows striking selectivity

between different anions. This supports our hypothesis that we can catalyse a range of reactions between anions in solution and substrates bound in the cage by exploiting different selectivity factors for the reacting partners.

RESULTS AND DISCUSSION

(i) Synthesis and crystallography of cages as halide salts.

Our recent work on guest binding in the cage cavity in water^{3d,11,14,15} has all been based on the cage \mathbf{H}^w (Fig. 1) that was designed to be water soluble through the presence of 24 hydroxymethyl groups on the exterior surface.¹⁵ This made the ligand synthesis considerably more difficult and time consuming than for the parent unsubstituted cage \mathbf{H} (which is insoluble in water as the BF_4^- salt).¹⁶ To simplify the preparation of a water-soluble version of the cage, and allow the straightforward preparation of larger amounts for a systematic study of its catalytic properties, we first investigated alternative strategies for increasing water solubility based on anion exchange.

Preparation of the unsubstituted cage directly as its chloride salt ($\mathbf{H}\cdot\text{Cl}_{16}$) from reaction of the free ligand \mathbf{L} with CoCl_2 was unsuccessful under a range of conditions. However we found that simply exchanging the $[\text{BF}_4]^-$ anions of $\mathbf{H}\cdot(\text{BF}_4)_{16}$ for chloride ions by ion exchange using Dowex resin could be effected whilst maintaining the structural integrity of the cage, allowing $\mathbf{H}\cdot\text{Cl}_{16}$ to be prepared easily. As its chloride salt, \mathbf{H} is highly water soluble without the need for the hydroxymethyl substituents on the ligands.¹⁵ An additional advantage of exchanging the anions is that this avoids the potential problem that, in water, $[\text{BF}_4]^-$ or $[\text{PF}_6]^-$ anions can undergo hydrolysis to liberate fluoride.¹⁷ For the work in this paper we needed to control which anions were present: replacing $[\text{BF}_4]^-$ with chloride as the anion removes any uncertainty in this respect as well as greatly simplifying the synthesis.

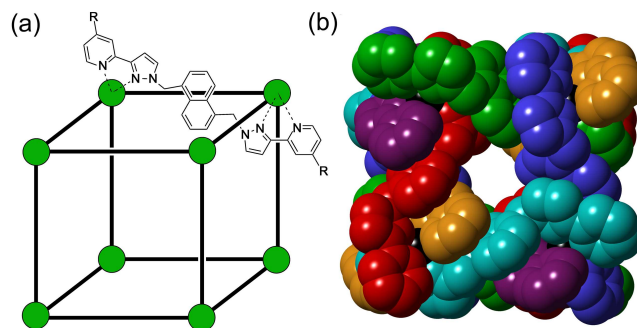


Figure 1. The host cages $[\text{Co}_8\text{L}_{12}](\text{BF}_4)_{16}$ for which the cage cations are abbreviated as \mathbf{H} ($\text{R} = \text{H}$) and \mathbf{H}^w ($\text{R} = \text{CH}_2\text{OH}$). (a) A sketch emphasising the cubic array of $\text{Co}(\text{II})$ ions and the disposition of one bridging ligand; (b) a view of the complex cation \mathbf{H} from a crystal structure with each ligand coloured separately for clarity.

Crystals of the chloride salt $\mathbf{H}\cdot\text{Cl}_{16}$, were grown from aqueous solution; the structure is in Fig. 2 (see ESI). The octanuclear cage cation has the same core structure as numerous previous examples of salts of both \mathbf{H} and \mathbf{H}^w ,^{3d,11,14-16,18} with two *fac* and six *mer* tris-chelate vertices, an inversion centre, and (non-crystallographic) S_6 symmetry. Significantly, all of the windows in the cage surface contain a chloride ion. These surface sites, as we have noted earlier, are invariably the

favoured positions for anions in different salts of **H** or **H^w**,^{3d,11,14-16,18} and observation of the chloride ions at these sites is consistent with the strongly inhibiting effect for the catalysed Kemp elimination, as they will displace the hydroxide ions whose surface binding is crucial for the catalysis.¹¹ The diameter of a chloride ion (3.3 Å) is slightly less than the diameter of each window which results in each surface-bound chloride ion being disordered over two closely-spaced positions. Each surface-bound chloride anion is involved in a range of CH•••Cl interactions with ligand fragments around the windows (Fig. 2, right).

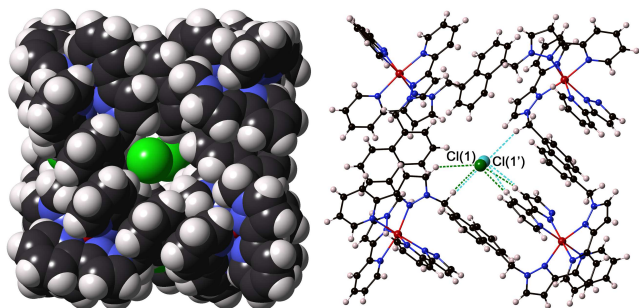


Figure 2. Two views of the crystal structure of **H•Cl₁₆**. Left: space-filling view of one face of the complex cation showing the presence of a chloride ion in the window (only one disorder component shown); all faces are symmetrically equivalent. Right: ball-and-stick view from the same perspective showing only one face of the cage. This illustrates the closest contacts between the chloride ion [disordered over two closely adjacent sites, Cl(1) (dark green) and Cl(1') (cyan)] and the surrounding set of CH groups; dashed lines indicate Cl•••HC contacts of ≤ 3.1 Å.

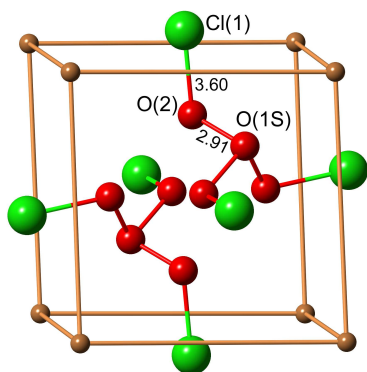


Figure 3. A view of the network of eight water molecules in the cavity of **H•Cl₁₆**. This is a simplified representation as both Cl(1) and O(2) exhibit positional disorder over closely spaced sites with only one component of each shown. Cl•••O and O•••O distances shown are in Å.

In contrast to other members of our cage family which commonly have anions located in the interior cavity as well as, or instead of, around the surface,¹⁹ the cavity of **H•Cl₁₆** contains only water molecules. There are two [O(1S), each with 100% occupancy] in each of the usual binding pockets on the interior surface associated with the convergence of CH protons around the *fac* tris-chelate binding pockets, at either end of the long diagonal.^{3d,11,14-16,18} Six more (crystallographically equivalent) water molecules O(2) form an approximately octahedral array, with each one involved in

an OH•••Cl hydrogen-bonding interaction with a chloride ion in one of the windows as well as being within hydrogen-bonding distance of O(1S). Each of these six water molecules is modelled as disordered over three closely-spaced sites, and this (together with the positional disorder of the chloride ions) means that any analysis of hydrogen-bonding distances between chloride ions and water molecules in the cavity is inappropriate. However it is clear that there is a network of eight water molecules inside the cage cavity with OH•••O interactions between them, further stabilised by interaction with either the H-bond donor sites on the cage interior surface [O(1S)], or the surface-bound chloride ions [O(2)] as shown in Fig. 3. Such networks of water molecules in the cavities of synthetic hosts provide part of the hydrophobic contribution to guest binding when they are liberated.²⁰

We also isolated and structurally characterised **H•(BF₄)I₁₅** to see if the pattern of anion binding to the cage windows is preserved for differently sized halides (see ESI). These crystals were prepared from single crystals of **H•(BF₄)₁₆** simply by soaking them in a methanolic solution of Bu₄NI for 24h; this resulted in partial anion exchange (fifteen of the sixteen fluoroborate anions are replaced by iodides) whilst retaining crystallinity. Several repeat experiments resulted in the same formulation, with one fluoroborate anion being retained but the other fifteen being replaced.

The crystal structure of the cage complex cation, with its associated iodide anions, is in Figs. 4 and 5. We see the same structure as before for the complex cation, although with minor variations (1 – 2%) in Co•••Co separations along the edges of the cage (see SI). Again we see an octahedral arrangement of anions associated with the cage surface, with one iodide ion occupying the window in each face of the cage cation. The large ionic diameter of the iodide anion (4.1 Å) provides a better match for the window size than does chloride, with the result that the bound iodide ions are not disordered.

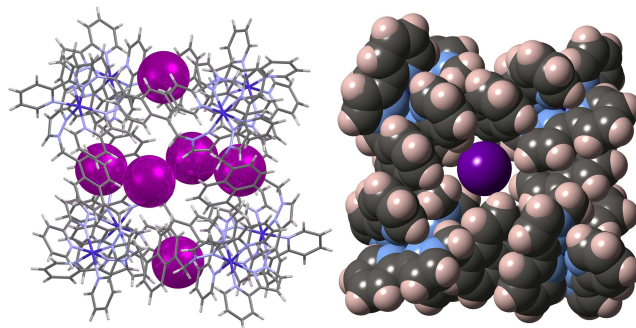


Figure 4. Two views of the crystal structure of **H•(BF₄)I₁₅**. Left: the complex cage cation (wireframe) and the surface-bound iodide anions (space-filling). Right: a space-filling view of one face emphasising the good fit of the iodide anion for the window in the cage surface.

The cavity contains six MeOH molecules (Fig. 5) of which four [O(1S), O(51S) and their symmetry equivalents, arranged in an approximate square] are hydrogen-bonded to iodide ions in the faces, with non-bonded O•••I distances of 3.50 – 3.51 Å. The remaining two encapsulated MeOH molecules [O(11S) and symmetry equivalent] interact with the usual H-bond donor sites on the cage interior surfaces at the diagonally opposed *fac* tris-chelate vertices.^{3d,11,14-16,18} The six

MeOH guests are arranged such that two equivalent pairs [O(11S) and O(51S)] are close together with an O...O separation of 2.83 Å, indicative of an OH...O hydrogen-bond between them. Thus, as with the water molecules in the interior of the chloride-based cage, the guest MeOH molecules are interacting with each other, with the cage interior surface, and with the surface-bound halide ions.

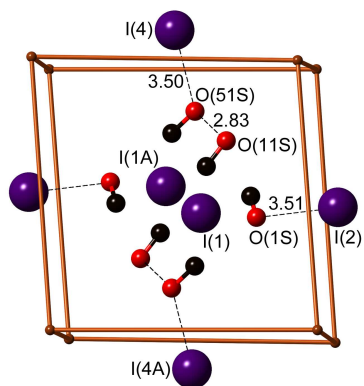


Figure 5. A view of the surface-bound anions of $\text{H}\cdot(\text{BF}_4)\text{I}_{15}$ and their interactions with the six MeOH guest molecules, with H-bonding interactions shown as dotted lines (O...O and O...I distances are in Å).

In both cases we suggest that the collection of weak but favourable CH... (anion) interactions in each cage window is the basis for accumulation of anions in these sites; it seems that the window size of this cage makes this favourable for a wide range of anions. We note that strong binding of anions in the central cavities of two-dimensional metal/ligand arrays such as cyclic helicates^{21,22} have been known since Lehn first reported the templating of a pentanuclear cyclic helicate by a chloride ion, giving a structure containing a strongly bound chloride that could not be removed with Ag(I) salts.²⁷

(ii) Effect of chloride concentration of the cage-catalysed reaction: onset of autocatalysis.

Under our standard conditions for NMR-based measurements,¹¹ a 1 mM solution of $\text{H}\cdot\text{Cl}_{16}$ catalyses the Kemp elimination about two orders of magnitude more slowly than $\text{H}\cdot(\text{BF}_4)_{16}$. This effect is associated with the chloride ions and not the presence or absence of external hydroxymethyl substituents, as conversion of the hydroxymethyl-functionalised cage to its chloride salt $\text{H}\cdot\text{Cl}_{16}$ resulted in a similar drop in catalytic activity. This observation that chloride ions suppress the catalytic of the cage is consistent with our previous report, where we showed that adding 47 mM LiCl reduces the observed rate of reaction to that of the background reaction.¹¹

To understand these effects in more detail, we investigated the effect of varying the concentration of chloride anions on the Kemp elimination catalysed by 1 mM $\text{H}\cdot\text{Cl}_{16}$ (D_2O , 298 K, 16 mM borate buffer, pD 10, 1.4 mM benzisoxazole). We varied the total concentration of chloride ions from 16 mM (the minimum, due to the cage counterions) to 48 mM by adding NaCl to the reaction mixture, and monitored the rate of the Kemp elimination reaction by ¹H NMR spectroscopy as described before.¹¹ The effect of added chloride on the rate of

reaction is shown in Fig. 6. These curves reveal two features: firstly, the initial rate of reaction is very sensitive to the concentration of chloride; and secondly, at higher concentrations of chloride, the progress curves are clearly sigmoidal in shape. The observation of inhibition as the chloride concentration increases is consistent with our previous suggestion that chloride competes strongly with DO^- for the sites at the cage surface in solution,¹¹ which is further supported by the crystal structure of $\text{H}\cdot\text{Cl}_{16}$ (above). The sigmoidal shape that appears on these curves as the chloride concentration increases to 48 mM suggests that the reaction becomes autocatalytic, with one of the products of the reaction catalysing the reaction.²³⁻²⁶

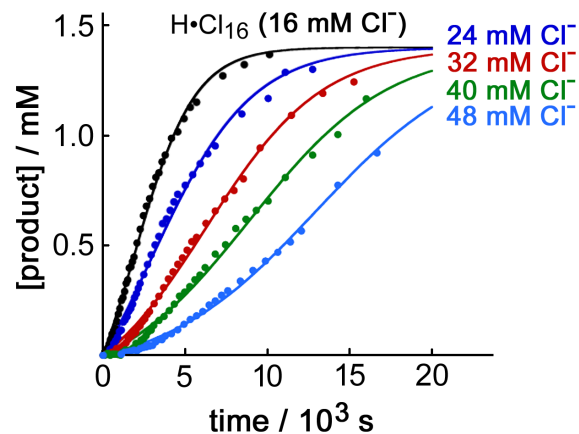


Figure 6. Reaction progress profiles showing the progress of the Kemp elimination in the presence of 1 mM $\text{H}\cdot\text{Cl}_{16}$ (D_2O , 298 K, 16 mM borate buffer, pD 10; black curve) and the effect of further increasing the concentration of Cl^- up to 48 mM.

Considering the autocatalytic behaviour, we note that the Kemp elimination reaction in solution is accurately first order in $[\text{DO}^-]$,¹¹ and that for the catalysed reaction the pH does not change significantly during the reaction (as expected for the buffered conditions that were used). Indeed, the reaction consumes base as the 2-cyanophenol product is deprotonated under our reactions conditions and so the acceleration as the reaction proceeds cannot be due to an increasing concentration of $[\text{DO}^-]$. Thus, the sigmoidal reaction profile is best explained by the 2-cyanophenolate anion acting as a base for the Kemp elimination and providing an additional reaction pathway as it accumulates.

Confirmation of this autocatalytic effect was provided by a series of experiments in which further 1.4 mM aliquots of the benzisoxazole were added to the reaction mixture and the continuing reaction monitored (Fig. 7). It is clear that as each aliquot of benzisoxazole is added, the sigmoidal profile is no longer evident and the reaction continues at a higher rate after each addition due to the increasing concentration of 2-cyanophenolate present. This behaviour is only evident in the presence of the chloride ions, which compete efficiently with hydroxide for the surface sites where the reaction occurs and so inhibit the hydroxide-based reaction (the chloride ions themselves are not sufficiently basic to catalyse the reaction). It appears that phenolate anions compete with hydroxide for these sites more efficiently than chloride anions do, because of their ‘softer’ nature and ease of desolvation, and this allows them to accumulate around the cage surface and catalyse the reaction due to their basicity. Importantly, control experi-

ments under identical conditions but in the absence of cage showed that additional aliquots of 2-cyanophenolate resulted in no change to the rate of the background (uncatalysed) Kemp elimination; autocatalysis requires *both* cyanophenolate and cage **H**. The order of preference for binding to the cage surface sites is therefore phenolate (which is basic enough to participate in the reaction, resulting in autocatalysis as it accumulates) > chloride (which just inhibits the reaction as it blocks access of the substrate to hydroxide and is a poor base) > hydroxide (the normal reaction pathway). **NMR titration experiments involving addition of portions of 2-cyanophenolate or chloride ions to a solution of $\text{H}\cdot\text{Cl}_{16}$ confirmed that the 2-cyanophenolate anions interact with the cage more strongly than do chloride ions (see SI).**

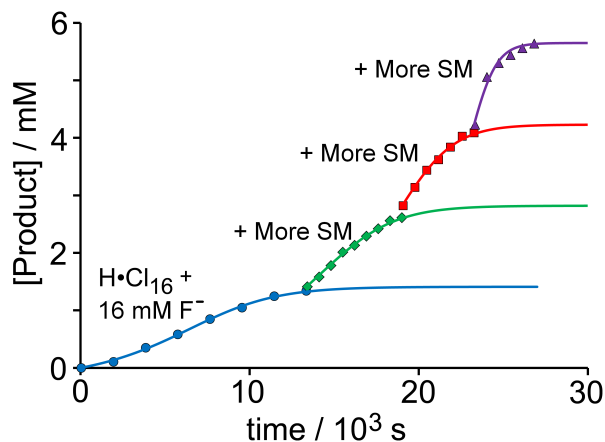


Figure 7. Experiment showing how the rate of the cage-catalysed Kemp elimination becomes faster with each additional 1.4 mM aliquot of starting material (SM) due to autocatalysis involving the 2-cyanophenolate product (for conditions, see main text).

We also explored the effect of adding similar amounts of different halide salts to the starting mixture to see the extent to which they inhibited the cage-catalysed Kemp reaction. With fluoride, it was clear that the extent of inhibition of the Kemp elimination compared to chloride follows what we might expect based on the Hofmeister series:²⁷ addition of 16 mM and then 32 mM F^- caused inhibition but had a much smaller effect than the same concentrations of Cl^- , presumably as F^- is more strongly hydrated and therefore has a lower affinity for the cage surface. In fact, in excess of 100 mM F^- is required to provide the same degree of inhibition as provided by an additional 32 mM Cl^- (Fig. 8; calculated rate constants for the 'normal' and autocatalytic reactions derived from these curves are tabulated in ESI and show how, as the concentration of halide ion increases, catalysis by the 'normal' route slows down allowing the autocatalytic pathway to become more dominant). With bromide and iodide, substantial inhibition (comparable to the effect achieved by adding 16 mM Cl^-) was observed with the addition of just < 2 mM of these ions. However, increasing the bromide / iodide concentration beyond this resulted in the solutions becoming turbid due to destruction of the cage and precipitation of free ligand as these ions are excellent ligands for Co(II).

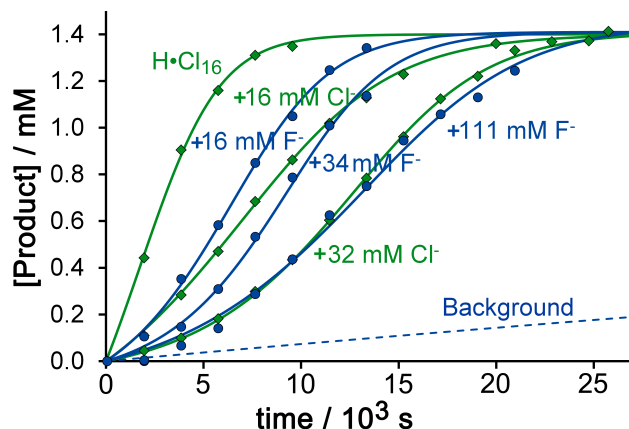


Figure 8. Comparison of the inhibiting effect on the cage-catalysed Kemp elimination of added fluoride (blue curves) compared to chloride (green curves), starting from $\text{H}\cdot\text{Cl}_{16}$ in each case (for conditions, see main text).

(iii) Involvement of other phenolate anions in the cage-catalysed Kemp elimination.

Following these observations we decided to see whether other phenolate bases could participate in the cage-catalysed Kemp elimination. The phenolates we chose for these are shown in Fig. 9 and have pK_a values ranging from 4 – 9. The reactions were all performed at pD 10 in the presence of 1 mM $\text{H}\cdot\text{Cl}_{16}$ and 16 mM NaF, which slowed the reaction with hydroxide down sufficiently for the accelerating effect of the added phenolate anions to be clear. The resultant reaction rate profiles in the presence of each different phenolate, and with no added phenolate, are summarised in Fig. 10.

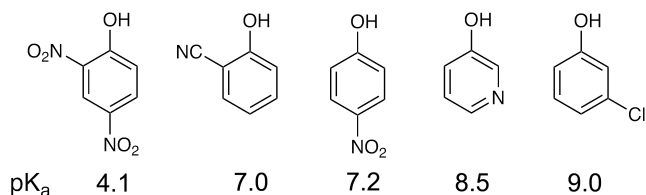


Figure 9. Series of phenols whose anions were used as bases for the catalysed Kemp elimination at pD = 10.

The dashed blue line in Fig. 10 shows the reaction progress with no additional phenolate present, but in the presence of 16 mM fluoride so that reaction with hydroxide is suppressed and the autocatalytic pathway is more apparent. It is clear from the reaction rate profiles in the presence of all of the added phenols in this series (with the exception of 2,4-dinitrophenol, which is discussed separately) that the presence of the relevant phenolate anion accelerates the catalysed Kemp elimination reaction. This is consistent with the previous suggestion that the phenolate anion accumulates around the cage surface in preference to DO^- , in the same way as chloride does, but can also act as a base.

The magnitude of the phenolate-induced rate acceleration correlates with increasing pK_a of the relevant phenol, *i.e.* with the basicity of the phenolate anion, with 3-chlorophenolate (pK_a 9 for the parent phenol) causing the greatest rate acceleration, about four times higher than that

provided by 2-cyanophenolate (pK_a 7). Of course there are two effects at work here simultaneously: (i) the increased *basicity* of the added phenolate anion which will enable it to deprotonate the bound benzisoxazole substrate more efficiently, and (ii) its ability to bind to the cage surface which is related to the ease with which it can be desolvated. The fact that the most basic phenolate anion has the largest effect on the catalysed reaction indicates that the former effect is dominant, which is reasonable given the structural similarities across the series.

As a control experiment we repeated the reaction under the conditions where it is accelerated by addition of 3-chlorophenolate (Fig. 10, green curve) but part-way through the reaction added cycloundecanone as an inhibitor.^{11,14} This binds much more strongly in the cage cavity than benzisoxazole but has itself no effect on the Kemp elimination; after addition of cycloundecanone the catalysed reaction stopped with no additional 2-cyanophenolate forming beyond the very slow contribution from the uncatalysed background reaction, because the benzisoxazole was displaced from the cage cavity (see SI). This confirms that the autocatalytic reaction pathway, like the previously-reported reaction pathway involving hydroxide as base,¹¹ requires *both* the substrate to be bound in the cage cavity *and* accumulation of the phenolate product around the cage surface. Consistent with this, if cycloundecanone were present at the start of the reaction using the conditions of Fig. 10 with 3-chlorophenolate present, the catalysed Kemp elimination was shut down entirely.

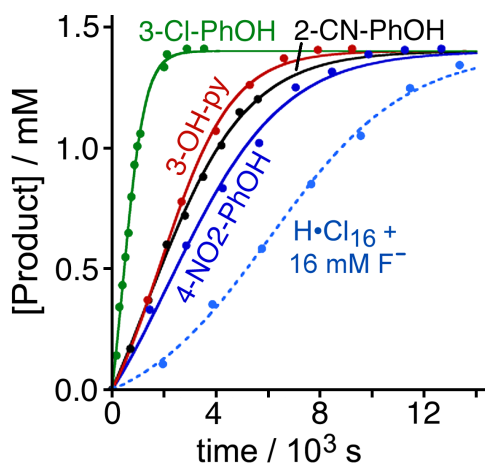


Figure 10: Rate profiles of the catalysed Kemp elimination by $\text{H}\cdot\text{Cl}_{16}$ at $\text{pD} = 10$ in the presence of 16 mM added fluoride (blue dashed line), and then with addition of 1.8 mM 4-nitrophenol (blue), 2-cyanophenol (black), 3-hydroxypyridine (red) and 3-chlorophenol (green).

The anomaly amongst this series of phenolates used (Fig. 9) is 2,4-dinitrophenol. This behaved differently from the other phenolate anions, shutting down the Kemp elimination reaction to uncatalysed background levels when added to the reaction. According to changes observed in the ^1H NMR spectrum of the cage in the presence of this phenol, the 2,4-dinitrophenolate anion binds inside the cage cavity, and so inhibits the reaction by competitive displacement of benzisoxazole (like cycloundecanone does). Normally we expect that charged species will not bind in the cage cavity in water due to the hydrophilicity induced by the charge;^{3d} protonation of neu-

tral amine guests or deprotonation of neutral carboxylic acid guests results in a decrease in their binding constant by 2 – 3 orders of magnitude and their ejection from the cage cavity.^{3d} However, in the 2,4-dinitrophenolate anion, the negative charge is extensively delocalised over the two nitro groups which reduces its hydrophilicity enough for it to bind inside the cavity ($K = 70 \text{ M}^{-1}$ for the anion, *cf.* 540 M^{-1} for neutral 2,4-dinitrophenol).

At the concentrations of chloride that we are able to use without causing decomposition of the cage, catalysis by 3-chlorophenolate is insensitive to chloride inhibition, unlike the background (hydroxide) promoted reaction. While increasing the concentration of chloride from 16 to 48 mM has a large effect on the reaction profile, the presence of 1.8 mM 3-chlorophenolate leads to reaction profiles that are essentially identical at substantially different chloride concentrations (Fig. 11). This confirms what we suggested earlier, *viz.* that chloride binds much more tightly than hydroxide and inhibits the reaction, but phenolate binds more tightly still, displacing chloride from the cage surface and restoring the reaction by the alternative autocatalytic pathway, at which point differences in the chloride concentration become irrelevant (red and green curves in Fig. 11).

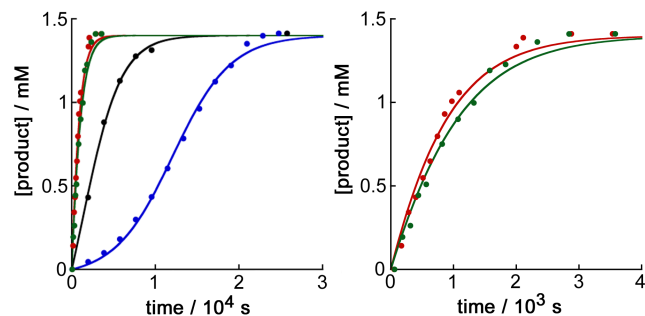


Figure 11: Reaction progress profiles showing the progress of the Kemp elimination in the presence of 1 mM $\text{H}\cdot\text{Cl}_{16}$ (D_2O , 298 K, 16 mM borate buffer, $\text{pD} = 10$; black curve); with 32 mM added Cl^- (blue curve, *cf.* pale blue line in Fig. 6); with 1.8 mM added 3-chlorophenolate (red curve); and with both 32 mM added Cl^- and 1.8 mM 3-chlorophenolate (green curve). The right-hand panel is an expansion of the red and green curves from the left-hand panel during the early part of the reaction.

Returning to the sensitivity of the initial rate of reaction to the chloride concentration (before autocatalysis by the phenolate product dominates), the observed rate constant for the initial reaction can be plotted against the total concentration of chloride (Fig. 12). This reveals that the sensitivity to chloride ion concentration is much greater than first order, and can actually be fit to a third order dependence (black line in Fig. 12); the fits of the data to second- or first-order dependence on chloride concentration are much less good.

This is striking as it suggests some form of cooperativity in the effect of chloride binding. Anion binding itself could be cooperative, with three chloride ions binding simultaneously to provide a catalytically inactive cage: although there are of course six windows (and hence anion binding sites) in a cage complex, it is possible that binding of chloride ions to a subset of these closest to the bound guest is sufficient to inhibit substantially the reaction with hydroxide. We note from the crystal structures of both $\text{H}\cdot\text{Cl}_{16}$ and $\text{H}\cdot\text{I}_{15}(\text{BF}_4)$ that

the halide ions that occupy the face centres are involved in hydrogen-bonding with an internal array of solvent molecules, and this could provide a rationale for cooperativity, with the presence of one face-bound chloride ion initiating ordering of the bound water molecules in the cage cavity in a way that facilitates cooperative binding of additional chloride ions at different windows by optimising hydrogen-bonding. An alternative possibility is that binding of anions to the cage is independent, but binding of just one anion is sufficient to prevent catalysis, which could happen if the first anion bound inside the cage cavity in solution at the site normally occupied by a guest. Whilst the reason for this high sensitivity of catalysis to amount of added chloride is not obvious, the evidence for the effect (Fig. 12) is quite clear.

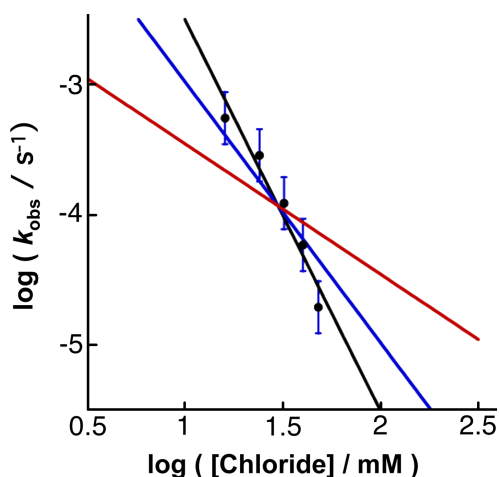


Figure 12: Variation in the rate constant for the Kemp elimination catalysed by 1 mM $\text{H}\cdot\text{Cl}_{16}$ (D_2O , 298 K, 16 mM borate buffer, pD 10) with total chloride ion concentration. The solid black line is the best fit for a third order relationship between inhibition and chloride ion concentration; blue and red lines are the best fits to second- and first-order dependence, respectively.

CONCLUSION

In conclusion, we have demonstrated that our previous observation of accumulation of hydroxide ions around the surface of a cationic coordination cage, which led to large increases in the rate of the Kemp elimination reaction of bound benzisoxazole,¹¹ is potentially general with other anions able to accumulate around the cage surface and displace hydroxide to an extent that depends on their ease of desolvation ($\text{HO}^- < \text{F}^- < \text{Cl}^- < \text{phenolates}$). As the reaction becomes more and more inhibited by added halide anions an unexpected autocatalytic pathway becomes apparent, with the product (2-cyanophenolate) starting to act as the base as it accumulates around the cage surface, displacing chloride more effectively than hydroxide does and able to act as a base. This autocatalytic route for the reaction is not normally visible because the reaction with hydroxide is much faster; but when the reaction with hydroxide is switched off by accumulation of the chloride or cyanophenolate anions around the cage, the autocatalytic route dominates. The ability of different phenolates to accelerate the catalysed reaction in the same way correlates with their basicity. Fig 13 illustrates the step in the proposed reaction cycle when 2-cyanophenolate is present that is responsible for the autocatalysis.

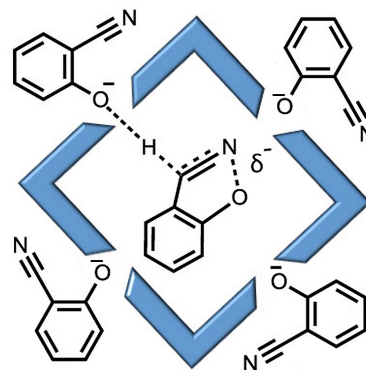


Figure 13. Autocatalysis of the Kemp elimination in the cage **H**.

Overall the demonstration that anions other than hydroxide can, under the correct conditions, be induced to be reaction partners with a cavity-bound guest is a significant step towards the goal of using these cages as general catalysis for reactions of electrophilic, cavity-bound guests with surface-bound anions.

ACKNOWLEDGEMENTS

We thank EPSRC and the Leverhulme Trust for financial support.

ASSOCIATED CONTENT

Supporting Information

The Supporting Information is available free of charge on the ACS Publications website.

Crystallographic data for $\text{H}\cdot\text{Cl}_{16}$ and $\text{H}\cdot(\text{BF}_4)\text{I}_{15}$ (CIFs).

Experimental details, sample NMR data illustrating the catalytic processes, and summary of crystallographic parameters (PDF).

AUTHOR INFORMATION

Corresponding Authors

* m.d.ward@warwick.ac.uk

* n.h.williams@sheffield.ac.uk

ORCID

Michael D. Ward: 0000-0001-8175-8822

Nicholas H. Williams: 0000-0002-4457-4220

Author Contributions

The manuscript was written through contributions of all authors. All authors have given approval to the final version of the manuscript.

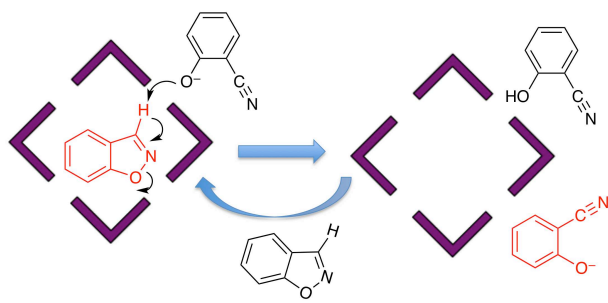
Funding Sources

EPSRC grants EP/L505055/1, EP/J00124/1, and EP/N031555/1; Leverhulme Trust grant RPG-2013-308

REFERENCES

- (a) Chakrabarty, R. J.; Mukherjee, P. S.; Stang, P. J. *Chem. Rev.* **2011**, *111*, 6810; (b) Zhang, Y.-Y.; Gao, W.-X.; Lin, L.; Jin, G.-X. *Coord. Chem. Rev.* **2017**, *344*, 323; (c) Cook, T. R.; Zheng, Y.-R.; Stang, P. J. *Chem. Rev.* **2013**, *113*, 734; (d) Pluth, M. D.; Bergman, R. G.; Raymond, K. N. *Acc. Chem. Res.* **2009**, *42*, 1650; (e) Smulders, M. M. J.; Riddell, I. A.; Browne, C.; Nitschke, J. R. *Chem. Soc. Rev.*

- 2013, 42, 1728; (f) Zarra, S.; Wood, D. M.; Roberts, D. A.; Nitschke, J. R. *Chem. Soc. Rev.* **2015**, 44, 419; (g) Vardhan, H.; Yusubov, M.; Verpoort, F. *Coord. Chem. Rev.* **2016**, 306, 171; (h) Schmidt, A.; Casini, A.; Kuhn, F. E. *Coord. Chem. Rev.* **2014**, 275, 19; (i) Cus-telcean, R. *Chem. Soc. Rev.* **2014**, 43, 1813; (j) Han, M.; Engelhard, D. M.; Clever, G. H. *Chem. Soc. Rev.* **2014**, 43, 1848; (k) Amouri, H.; Desmaretz, C.; Moussa, J. *Chem. Rev.* **2014**, 112, 2015; (l) Yoshizawa, M.; Yamashina, M. *Chem. Lett.* **2017**, 46, 163; (m) Ward, M. D.; Hunter, C. A.; Williams, N. H. *Chem. Lett.* **2017**, 46, 2.
- (2) Ward, M. D.; Raithby, P. R. *Chem. Soc. Rev.* **2013**, 42, 1619.
- (3) (a) Garci, A.; Mbakidi, J.-P.; Chaleix, V.; Sol, V.; Orhan, E.; Therrien, B. *Organometallics* **2015**, 34, 4138; (b) Therrien, B. *Chem. Eur. J.* **2013**, 19, 8378; (c) Lewis, J. E. M.; Gavey, E. L.; Cameron, S. A.; Crowley, J. D. *Chem. Sci.* **2012**, 3, 778; (d) Cullen, W.; Turega, S.; Hunter, C. A.; Ward, M. D. *Chem. Sci.* **2015**, 6, 625.
- (4) (a) Furutani, Y.; Kandori, H.; Kawano, M.; Nakabayashi, K.; Yoshizawa, M.; Fujita, M. *J. Am. Chem. Soc.* **2009**, 131, 4764; (b) Murase, T.; Nishijima, Y.; Fujita, M. *Chem. Asian J.* **2012**, 2, 826; (c) Murase, T.; Takezawa, H.; Fujita, M. *Chem. Commun.* **2011**, 47, 10960; (d) Gera, R.; Das, A.; Jha, A.; Dasgupta, J. *J. Am. Chem. Soc.* **2014**, 136, 15909; (e) Jing, X.; He, C.; Yang, Y.; Duan, C. *J. Am. Chem. Soc.* **2015**, 137, 3967; (f) Dalton, D. M.; Ellis, S. R.; Nichols, E. M.; Mathies, R. A.; Toste, F. D.; Bergman, R. G.; Raymond, K. N. *J. Am. Chem. Soc.* **2015**, 137, 10128; (g) Ward, M. D. in Atwood, J. L. (ed.) *Comprehensive Supramolecular Chemistry II*, **2017**, 6, 357 (Elsevier, Oxford, UK).
- (5) (a) Brown, C. J.; Toste, F. D.; Bergman, R. G.; Raymond, K. N. *Chem. Rev.* **2015**, 115, 3012; (b) Ajami, D.; Rebek, J., Jr. *Acc. Chem. Res.* **2013**, 46, 990; (c) Yoshizawa, M.; Klosterman, J. K.; Fujita, M. *Angew. Chem., Int. Ed.* **2009**, 48, 3418.
- (6) Kang, J.; Rebek, J. Jr. *Nature* **1997**, 385, 50.
- (7) Yoshizawa, M., Tamura & M., Fujita, M. *Science* **2006**, 312, 251.
- (8) Kaphan, D. M.; Toste, F. D.; Bergman, R. G.; Raymond, K. N. *J. Am. Chem. Soc.* **2015**, 137, 9202.
- (9) Hastings, C. J.; Pluth, M. D.; Bergman, R. G.; Raymond, K. N. *J. Am. Chem. Soc.* **2010**, 132, 6938.
- (10) (a) Pluth, M. D.; Bergman, R. G.; Raymond, K. N. *J. Org. Chem.*, **2009**, 74, 58; (b) Pluth, M. D.; Bergman, R. G.; Raymond, K. N. *Science*, **2007**, 316, 85.
- (11) Cullen, W.; Misuraca, M. C.; Hunter, C. A.; Williams, N. H.; Ward, M. D. *Nat. Chem.* **2016**, 8, 231.
- (12) (a) Casey, M. L., Kemp, D. S., Paul, K. G. & Cox, D. D. *J. Org. Chem.* **1973**, 38, 2294; (b) Kemp, D. S., Casey, M. L. *J. Am. Chem. Soc.* **1973**, 95, 6670.
- (13) Marcus, Y. *J. Chem. Soc., Faraday Trans.* **1991**, 87, 2995.
- (14) (a) Turega, S.; Cullen, W.; Whitehead, M.; Hunter, C. A.; Ward, M. D. *J. Am. Chem. Soc.* **2014**, 136, 8475; (b) Cullen, W.; Turega, S.; Hunter, C. A.; Ward, M. D. *Chem. Sci.* **2015**, 6, 2790; (c) Taylor, C. G. P.; Cullen, W.; Collier, O. M.; Ward, M. D. *Chem. Eur. J.* **2017**, 23, 206.
- (15) Whitehead, M.; Turega, S.; Stephenson, A.; Hunter, C. A.; Ward, M. D. *Chem. Sci.* **2013**, 4, 2744.
- (16) Tidmarsh, I. S.; Faust, T. B.; Adams, H.; Harding, L. P.; Russo, L.; Clegg, W.; Ward, M. D. *J. Am. Chem. Soc.* **2008**, 130, 15167.
- (17) Freire, M. G.; Neves, C. M. S. S.; Marrucho, I. M.; Coutinho, J. A. P.; Fernandes, A. M. J. *Phys. Chem. A* **2009**, 114, 3744.
- (18) Turega, S.; Whitehead, M.; Hall, B. R.; Haddow, M. F.; Hunter, C. A.; Ward, M. D. *Chem. Commun.* **2012**, 48, 2752; (b) Turega, S.; Whitehead, M.; Hall, B. R.; Meijer, A. J. H. M.; Hunter, C. A.; Ward, M. D. *Inorg. Chem.* **2013**, 52, 1122.
- (19) Ward, M. D. *Chem. Commun.* **2009**, 4487.
- (20) (a) Biedermann, F.; Nau, W. M.; Schneider, H.-J. *Angew. Chem., Int. Ed.* **2014**, 53, 11158; (b) Metherell, A. J.; Cullen, W.; Williams, N. H.; Ward, M. D. *Chem. Eur. J.* in press (DOI: 10.1002/chem.201704163).
- (21) Hasenknopf, B.; Lehn, J.-M.; Kneisel, B. O.; Baum, G.; Fenske, D. *Angew. Chem., Int. Ed.* **1996**, 35, 1838-1840.
- (22) (a) Campos-Fernandez, C. S.; Schottel, B. L.; Chifotides, H. T.; Bera, J. K.; Bacsá, J.; Koomen, J. M.; Russell, D. H.; Dunbar, K. R. *J. Am. Chem. Soc.* **2005**, 127, 12909; (b) Riddell, I. A.; Smulders, M. M. J.; Clegg, J. K.; Hristova, Y. R.; Breiner, B.; Thoburn, J. D.; Nitschke, J. R. *Nat. Chem.* **2012**, 4, 751; (c) Argent, S. P.; Adams, H.; Riis-Johannessen, T.; Jeffery, J. C.; Harding, L. P.; Mamula, O.; Ward, M. D. *Inorg. Chem.* **2006**, 45, 3905.
- (23) (a) Bissette, A. J.; Fletcher, A. J. *Angew. Chem., Int. Ed.* **2013**, 52, 12800; (b) Vidonne, A.; Philp, D. *Eur. J. Org. Chem.* **2009**, 593.
- (24) (a) Nowick, J. S.; Feng, Q.; Tjivukia, T.; Ballester, P.; Rebek, J. Jr. *J. Am. Chem. Soc.* **1991**, 113, 8831; (b) Rotello, V.; Hong, J.-I.; Rebek, J. Jr. *J. Am. Chem. Soc.* **1991**, 113, 9422; (c) Wintner, E. A.; Conn, M. M.; Rebek, J. Jr. *J. Am. Chem. Soc.* **1994**, 116, 8877; (d) Kamioka, S.; Ajami, D.; Rebek, J. Jr. *Proc. Natl. Acad. Sci. USA* **2010**, 107, 541.
- (25) (a) von Kiedrowski, G. *Bioorg. Chem. Front.* **1993**, 3, 113-146; (b) Stahl, I.; von von Kiedrowski, G. *J. Am. Chem. Soc.* **2006**, 128, 14014; (c) Kindermann, M.; Stahl, I.; Reimold, M.; Pankau, W. M.; von Kiedrowski, G. *Angew. Chem., Int. Ed.* **2005**, 44, 6750.
- (26) (a) Allen, V. C.; Philp, D.; Spencer, N. *Org. Lett.* **2001**, 3, 777; (b) Kassianidis, E.; Pearson, R. J.; Philp, D. *Org. Lett.* **2005**, 7, 3833; (c) Sadownik, J. W.; Philp, D. *Angew. Chem., Int. Ed.* **2008**, 47, 9965; (d) Bottero, I.; Huck, J.; Kosikova, T.; Philp, D. *J. Am. Chem. Soc.* **2016**, 138, 6723.
- (27) Xie, W.-J.; Gao, Y. Q. *J. Phys. Chem. Lett.* **2013**, 4, 4247.



Insert Table of Contents artwork here